CANCER GENOMICS & PROTEOMICS *13*: 493-498 (2016)
doi:10.21873/cgp.20012

Introduction of *ID2* Enhances Invasiveness in *ID2*-null Oral Squamous Cell Carcinoma Cells *via* the SNAIL Axis

YU KAMATA[1], TOMOKI SUMIDA[1], YOSUKE KOBAYASHI[1], AKIKO ISHIKAWA[2], WATARU KUMAMARU[1] and YOSHIHIDE MORI[1]

[1]*Section of Oral & Maxillofacial Surgery, Division of Maxillofacial Diagnostic and Surgical Sciences, Faculty of Dental Science, Kyushu University, Fukuoka, Japan;*
[2]*Department of Oral and Maxillofacial Surgery, Ehime University Graduate School of Medicine, Ehime, Japan*

Abstract. *Aim: Inhibitor of DNA-binding (ID) proteins are negative regulators of basic helix-loop-helix transcription factors that generally stimulate cell proliferation and inhibit differentiation. However, the role of ID2 in cancer progression remains ambiguous. Here, we investigated the function of ID2 in ID2-null oral squamous cell carcinoma (OSCC) cells. Materials and Methods: We introduced an ID2 cDNA construct into ID2-null OSCC cells and compared them with empty-vector-transfected cells in terms of cell proliferation, invasion, and activity and expression of matrix metalloproteinase (MMP). Results: ID2 introduction resulted in enhanced malignant phenotypes. The ID2-expressing cells showed increased N-cadherin, vimentin, and E-cadherin expression and epithelial–mesenchymal transition. In addition, cell invasion drastically increased with increased expression and activity of MMP2. Immunoprecipitation revealed a direct interaction between ID2 and zinc finger transcription factor, snail family transcriptional repressor 1 (SNAIL1). Conclusion: ID2 expression triggered a malignant phenotype, especially of invasive properties, through the ID2– SNAIL axis. Thus, ID2 represents a potential therapeutic target for OSCC.*

Basic helix-loop-helix (bHLH) transcription factors are key regulators of lineage- and tissue-specific gene expression in mammalian and non-mammalian organisms (1). bHLH proteins act as obligate dimers and dimerize through their HLH domains and bind DNA through their composite basic domains, regulating the transcription of target genes containing E-boxes (CANNTG) in their promoters (2). Inhibitor of DNA-binding (ID) proteins can dimerize with bHLH proteins. ID–bHLH heterodimers fail to bind DNA as the ID proteins lack basic domains. Thus, ID proteins are dominant negative regulators of the function of bHLH proteins (2).

Constitutive ID protein expression of has been shown to inhibit the differentiation of various cell types (3, 4). Four subtypes of the *ID* gene family have been described thus far: *ID1, ID2, ID3*, and *ID4*. The different members of the ID family show varying expression patterns and functions and localize to different chromosomes (5, 6). Previously, we investigated the role of the ID1 protein in oral squamous cell carcinoma (OSCC), which is the most common type of oral cancer, and found that ID1 plays an important role during cancer cell progression (7). *ID1* is expressed during proliferation and can suppress differentiation in all cell types examined so far; however, the data on *ID2* are much less consistent. While the HLH motif of ID2 is similar to that of ID1 (8, 9), the remainders of the sequence are considerably different. Both proteins are encoded by different genes. Similarly to *ID1, ID2* was first identified as an inhibitor of differentiation because it is down-regulated during the differentiation of various cell types (4, 10). In addition, *ID2* overexpression inhibits myoblast differentiation (11) and blocks stage-specific development early in thymopoiesis (12). Moreover, the expression of both *ID1* and *ID2* is up-regulated during prostate cancer progression (13). However, inconsistent with its role as a differentiation inhibitor, *ID2* levels have been shown to substantially increase during the differentiation of myeloid precursors such as HL-60 cells into granulocytes or macrophages (14). *ID2* expression is also maintained during embryonic stem cell-derived hematopoietic differentiation (15). Mice deficient in ID2 are devoid of lymph nodes and Peyer's patches and exhibit disturbed differentiation of natural killer cells (16).

Correspondence to: Dr. Tomoki Sumida, Section of Oral & Maxillofacial Surgery, Division of Maxillofacial Diagnostic and Surgical Sciences, Faculty of Dental Science, Kyushu University, 3-1-1, Maidashi, Higashi-ku, Fukuoka, 812-8582, Japan. Tel: +81 926426452, Fax: +81 926426392, e-mail: tomoki@dent.kyushu-u.ac.jp

Key Words: Inhibitor of differentiation, epithelial–mesenchymal transition, matrix metalloproteinase, invasion, SNAIL.

Based on this controversy regarding the role of *ID2* during cancer progression, we investigated its role in OSCC cells to determine whether it acts as a pro-differentiating agent or as a promoter of tumor cell aggressiveness. To this end, we generated *ID2*-overexpressing mutants and evaluated their proliferative and invasive capacities and matrix metalloproteinase (MMP) secretion.

Materials and Methods

Cell culture. The human OSCC cell line Ca9-22, originally derived from a patient with tongue cancer, was purchased from the American Tissue Culture Collection (Manassas, VA, USA). The cells were cultured in RPMI-1640 (Sigma-Aldrich, St. Louis, MO, USA) supplemented with 5% fetal bovine serum (FBS) at 37˚C in the presence of 5% CO_2.

Transfection of pBabe-ID2S. Full-length human *ID2* cDNA was excised from CMV-*ID2* and cloned into pBabe-puro (17) in sense orientation. pBabe-*ID2*S and pBabe-ctl (empty vector) were separately transfected into Ca9-22 cells using Lipofectamine® 2000™ Reagent (Life Technologies, Carlsbad, CA, USA). The cells were selected in 0.6 mg/ml puromycin. The transfected cells (Ca9-22-*ID2*S and Ca9-22-ctl) were then screened for ID2 protein expression.

Western blot analysis. The cells were lysed in Laemmli buffer and stored at −70˚C. Protein concentrations were determined using the DC protein assay kit (Bio-Rad, Hercules, CA, USA). Total protein samples (20-30 μg) were separated by sodium dodecyl sulphate–polyacrylamide gel electrophoresis and transferred to polyvinylidene difluoride membranes (Hybond® P; GE Healthcare, Amersham Buckinghamshire, UK). The membranes were then blocked for 1 h at room temperature with TBST (20 mM Tris, 137 mM NaCl, 3.8 mM HCl, and 0.1% Tween® 20) containing 5% non-fat milk and then probed with anti-ID1, anti-ID2, or anti-ID3 (Z-8, C-20, C-20; Santa Cruz Biotechnology, Santa Cruz, CA, USA), anti-E-cadherin (HECD-1; Abcam, Cambridge, UK), anti-N-cadherin (CL32; BD Biosciences, San Jose, CA, USA), anti-vimentin (V9; Dako, Glostrup, Denmark), anti-SNAIL (ab117866; Abcam), anti-p21 (C-19; Santa Cruz Biotechnology), anti-serine/threonine kinase 1 (protein kinase B, AKT) (610860; BD Biosciences Pharmingen, San Diego, CA, USA), anti-pAKT (Thr308) (558275; BD Biosciences Pharmingen), anti-pAKT (Ser473) (560404; BD Biosciences Pharmingen), anti-MMP2 (ab2462; Abcam), anti-MMP9 (ab35326; Abcam), or anti-actin (C4; EMD Millipore, Billerica, MA, USA) antibodies for 1 h. Next, the membranes were washed and incubated with a secondary antibody (either goat anti-rabbit or anti-mouse IgG-horseradish peroxidase) (Santa Cruz Biotechnology) overnight, washed again, and developed using enhanced chemiluminescence with the Amersham ECL-Plus kit according to the manufacturer's instructions (GE Healthcare).

MTT assay. To quantify cell proliferation, the 3-[4,5-dimethylthiazol-2-yl]-2,5-diphenyl tetrasodium bromide (MTT) assay was used (Chemicon International, Temecula, CA, USA). Cells were seeded in 96-well plates at 3×10^3 cells/well for 2 days. Upon completion of treatments, the cells were incubated at 37˚C with MTT for 4 h, and then isopropanol with 0.04 N HCl was added and the absorbance was read after 1 h in a plate reader with a test wavelength of 570 nm. The absorbance of the medium alone at 570 nm was subtracted, and the percentage viability relative to that of the control was calculated as the absorbance of the treated cells/control cells ×100.

Boyden chamber invasion assay. Invasion assays were performed in modified Boyden chambers with 8-μm-pore filter inserts for 24-well plates (Collaborative Research, Waltham, MA, USA). The filters were coated with 10-12 μl of ice-cold Matrigel (Collaborative Research). Ca9-22-*ID2*S and Ca9-22-ctl cells (40×10^3 cells/well) were then added to the upper chamber in 200 μl of serum-free medium. The lower chamber was filled with 300 μl of conditioned medium from fibroblasts. After incubation for 20 h, the cells were fixed with 2.5% glutaraldehyde in PBS and stained with 0.5% toluidine blue in 2% Na_2CO_3. Cells that remained in the Matrigel or were attached to the upper side of the filter were removed using cotton tips. Cells on the lower side of the filter were counted using light microscopy. Assays were performed in triplicate and the results were averaged.

Zymography. Proliferating Ca9-22-*ID2*S and Ca9-22-ctl cells (1×10^6 cells in 100-mm dishes) were shifted to serum-free media for 2-3 days, after which the medium was replaced with 10 ml of fresh serum-free medium. Forty-eight hours later, the conditioned medium was collected and concentrated 10- to 15-fold using 10-kDa cut-off filters (EMD Millipore, Billerica, MA, USA). The concentrated medium was then analyzed using gelatin substrate gels. The gels consisted of 8-10% polyacrylamide and 3 mg/ml gelatin (Sigma-Aldrich). Concentrated conditioned medium was mixed with non-reducing Laemmli sample buffer and incubated at 37˚C for 15 min. After electrophoresis, the gels were incubated for 1 h in 2.5% Triton™ X-100 at room temperature, followed by 24-48-h incubation in substrate buffer [100 mM Tris-HCl (pH 7.4) and 15 mM $CaCl_2$]. The gels were then stained with Coomassie Blue for 30 min and destained with 30% methanol/10% acetic acid.

Immunoprecipitation assay. The Ca9-22-ID2S and Ca9-22-ctl cells were lysed using lysis buffer (0.5% Nonidet P-40, 50 mM Tris-Cl, 10% glycerol, 0.1 M EDTA, and 15 mM NaCl), and whole-cell lysates were collected. Five micrograms of anti-SNAIL antibody or 2.0 μg of the appropriate control lgG was incubated with 500 μg of the lysates for 4 h at 4˚C. Fifty microliters of resuspended Protein A/G Plus Agarose (Santa Cruz Biotechnology) was added, and the mixture was again incubated at 4˚C overnight. The protein A/G Plus Agarose-bound immunocomplexes were washed several times with lysis buffer and analyzed by western blotting as described above.

Statistical analysis. Statistical comparisons were performed using the two-tailed Student *t*-test. A *p*-value of less than 0.05 was regarded as significant. SPSS version 22.0 (IBM, Armonk, NY, USA) was used for statistical analyses.

Results

Introduction of ID2 into the ID2-null Ca9-22 cells. The Ca9-22 cells were transfected with pBabe vector-containing sense full-length *ID2* cDNA or with empty vector as a control. Western blotting revealed that ID2 protein expression was increased in the Ca9-22-*ID2*S cells compared to that in the control and parental cells (Figure 1A). Ca9-22 cells showed no expression of ID1 and ID3. There was no induction of ID1 and *ID3* expression after *ID2*

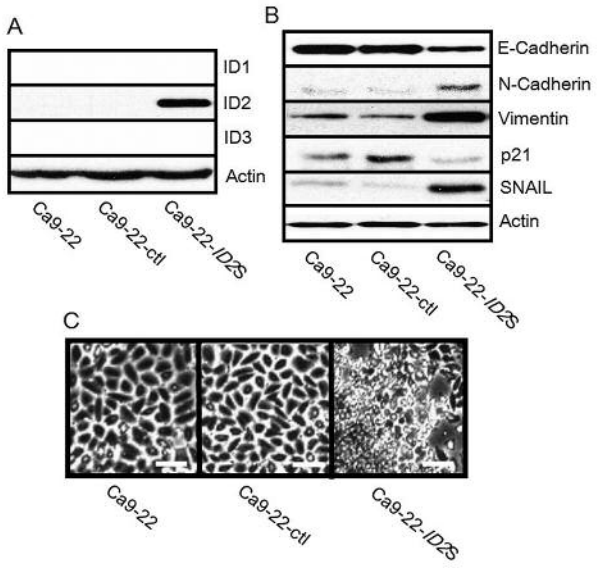

Figure 1. *Introduction of inhibitor of differentiation (ID)-2 and epithelial–mesenchymal transition. A: Expression of potential downstream genes upon up-regulation of ID2 in Ca9-22 cells. B: Western blot analysis of the expression of ID1, ID2 and ID3, as well as that of E-cadherin, N-cadherin, and vimentin in the three different cell populations, Ca9-22: Parental oral squamous cell carcinoma cell line; Ca9-22-ctl: parental cells transfected with empty vector; Ca9-22-ID2S: parental cells transfected with ID2 expression vector. Actin was used as a loading control. C: Representative images of Ca9-22, Ca9-22-ctl, and Ca9-22-ID2S cells taken using a microscope at a magnification of ×100. Scale bar=150 μm. SNAIL: Zinc finger transcription factor, snail family transcriptional repressor 1.*

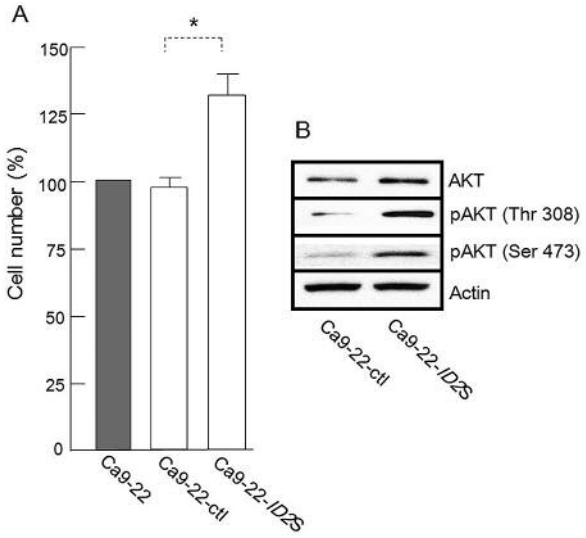

Figure 2. *Effect of inhibitor of differentiation 2 (ID2) expression on Ca9-22 cell proliferation and the serine/threonine kinase 1 (protein kinase B, AKT) pathway. A: Proliferation of the different cell populations as determined using the 3-[4,5-dimethylthiazol-2-yl]-2,5-diphenyl tetrasodium bromide assay. parental Ca9-22 cells transfected with ID2 expression vector (Ca9-22-ID2S) cells grew faster than parental cells and cells transfected with empty vector (Ca9-22-ctl) *Significantly different at $p<0.01$. B: Western blotting indicated that expression of phosphorylated (p) AKT (Thr308 and Ser473) was induced in Ca9-22-ID2S cells compared with Ca9-22-ctl cells.*

introduction. Next, we investigated the potential modulation of the expression of genes known to be either down-regulated (E-cadherin) or up-regulated (N-cadherin and vimentin) during epithelial–mesenchymal transition. The expression of both N-cadherin and vimentin was increased in Ca9-22-*ID2*S cells, while that of E-cadherin was decreased, indicating that *ID2* gene expression in these cancer cells can trigger epithelial–mesenchymal transition. *p21* was down-regulated and *SNAIL* expression was drastically induced (Figure 1B). Moreover, the cell shape also changed: the Ca9-22-*ID2*S cells were relatively small and grew in multilayers compared with the parental and control cells. However, the Ca9-22-ctl cells had a more flattened appearance and formed monolayers (Figure 1C).

Effect of ID2 gene modulation on cell proliferation and AKT phosphorylation. We found a significant difference in the rate of proliferation between the Ca9-22-*ID2*S and the Ca9-22-ctl cells (Figure 2A), with Ca9-22-*ID2*S cells being significantly more proliferative than the Ca9-22-ctl cells ($p<0.05$). Furthermore, introduction of the *ID2* gene resulted in AKT phosphorylation. Western blotting indicated that the quantity of pAKT (Thr308 and Ser473) was increased in Ca9-22 cells after *ID2* introduction (Figure 2B).

Effect of ID2 introduction on cell invasion and MMP secretion. One of the major features of aggressive and metastatic cancer cells is their ability to invade their microenvironment through the secretion of MMPs. Therefore, we first compared the invasive phenotype of the different cell populations using the Boyden chamber invasion assay. Invasiveness was strongly induced in the Ca9-22-*ID2*S cells ($p<0.01$) as compared to that in the Ca9-22-ctl cells (Figure 3A). Accordingly, the activity and expression of MMP2 and the secretion of MMP9 by the Ca9-22-*ID2*S cells was increased, but the activity and expression of these MMPs were undetectable in Ca9-22-ctl cells (Figure 3B), which could explain the strong induction of invasiveness in Ca9-22-*ID2*S cells.

Interaction of SNAIL with ID2. Immunoprecipitation indicated that ID2 interacts with SNAIL, which is the key player in the epithelial–mesenchymal transition. The level of interaction between SNAIL and ID2 paralleled the ID2 expression level (Figure 4).

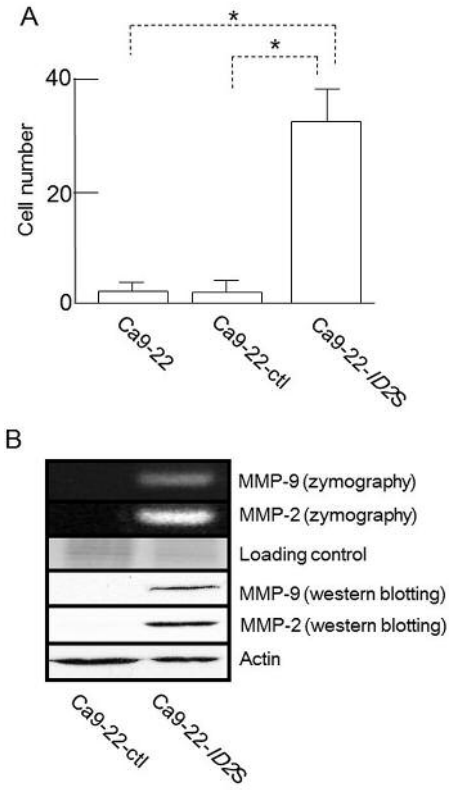

Figure 3. *Effect of inhibitor of differentiation 2 (ID2) expression on Ca9-22 cell (Ca9-22-ID2S) invasiveness and the activity and secretion of matrix metalloproteinase (MMP)-2 and MMP9. A: Cell counts of each population, as determined using Boyden chamber invasion assays. Invasive capacity was induced in Ca9-22-ID2S cells compared with cells transfected with empty vector (Ca9-22-ctl). *Significantly different at p<0.01. B: Gelatin zymography and western blotting revealed differences in MMP activity and expression. In particular, MMP2 was strongly up-regulated in Ca9-22-ID2S cells.*

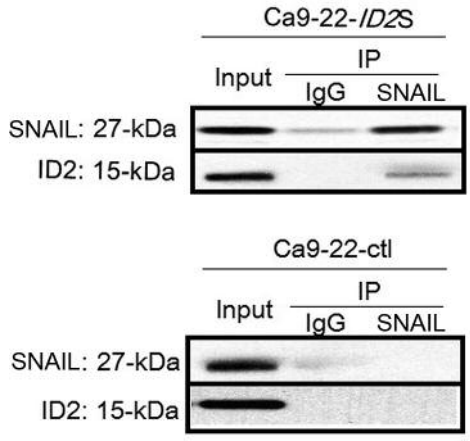

Figure 4. *Inhibitor of differentiation 2 (ID2)-bearing cells (Ca9-22-ID2S), zinc finger transcription factor, snail family transcriptional repressor 1 (SNAIL1) interacts with ID2 directly. Well-washed immunocomplexes derived from Ca9-22-ID2S cells and cells transfected with empty vector (Ca9-22-ctl) were prepared. Anti-SNAIL antibody or control IgG was used for immunoprecipitation (IP). Samples were analyzed by western blotting with anti-SNAIL and anti-ID2 antibodies. In Ca9-22-ID2S cells, direct interaction between SNAIL and ID2 was revealed.*

Discussion

In this study, the effect of *ID2* introduction on *ID2*-null OSCC cells was determined. In terms of cell proliferation, ID2 protein induced a malignant phenotype. ID2 is the only protein from the HLH family that can also physically interact with retinoblastoma protein (Rb) and prevent its antiproliferative activity. ID2 can also simultaneously control cell differentiation and cell-cycle progression (2, 18).

One of the major differences in *ID2*-overexpressing Ca9-22 cells was a change in cell shape. The Ca9-22-*ID2*S cells were highly disordered and formed multilayers, while the Ca9-22-ctl cells formed single layers. Moreover, the Ca9-22-*ID2*S cells exhibited a moderately increased invasive behavior compared to the control cell populations. MMP secretion was not detectable in the original and control cells, but a drastically increased activity and expression of MMP was observed in the cells with introduced *ID2*. In patients with hepatocellular carcinoma, increased expression levels of E-cadherin, ID2, and MMP9 are considered unfavorable prognostic factors (19). In particular, the expression of MMP2 was considerably induced.

We also speculated that *ID2* transfection might be able to stimulate the SNAIL–ID2 axis. In colorectal cancer cells, the suppression of E-cadherin expression through activation of SNAIL led to the activation of MMPs (20). Therefore, we performed immunoprecipitation experiments, that revealed a direct interaction between SNAIL and ID2. It was previously only suggested that ID2 interacts directly with SNAIL (21, 22), which is a zinc finger transcriptional repressor present in invasive carcinoma cell lines and tumors in which E-cadherin expression is lost (23). Epithelial–mesenchymal transition is a fundamental process that underlies cancer progression; however, to date, there are only few reports on the relationship between epithelial–mesenchymal transition and *ID2*. The expression of the epithelial–mesenchymal transition markers, E-cadherin, N-cadherin, and vimentin, was also different between the groups of cells in our study. Taken together, these data indicate that this interaction between SNAIL and *ID2* might induce epithelial–mesenchymal transition in OSCC.

The introduction of *ID2* expression triggered significant changes in the phenotype of the cells. However, the effect of *ID2* suppression needs to be investigated using OSCC cells with high malignancy in future studies. At least in OSCC cells, *ID2* expression not only follows a pattern similar to that of *ID1*, but also appears to be independent from other IDs during

OSCC progression. Based on our results, ID2 could act as an oncogenic protein in Ca9-22 cells, and we propose that the introduction of *ID2* could lead OSCC cells to a more aggressive phenotype and enhance their aggressiveness, especially their invasive property.

In summary, we found that ID2 acts as an inducer of cancer cell proliferation and invasion. ID2 also induces EMT, which is a fundamental process that underlies the progression of cancer. Our findings also indicate that ID2 is a unique member of the ID protein family that can function independently of ID1 or ID3. Based on our findings, we believe that targeting *ID2* gene expression might represent a novel therapeutic approach for OSCC.

Conflicts of Interest

All Authors declare no financial or other potential conflict of interest in regard to this study.

Acknowledgements

This work was supported by JSPS KAKENHI Grant Number 15K11257 and 16K20587. The authors gratefully acknowledge this financial support. The authors would also like to thank Editage for English language editing.

References

1 Huang C, Chan JA and Schuurmans C: Proneural bHLH genes in development and disease. Curr Top Dev Biol *110*: 75-127, 2014.
2 Benezra R, Davis RL, Lockshon D, Turner DL and Weintrau H: The protein ID: a negative regulator of helix-loop-helix DNA-binding proteins. Cell *61*: 49-59, 1990.
3 Norton JD, Deed RW, Craggs G and Sablitzky F: ID helix-loop-helix proteins in cell growth and differentiation. Trends Cell Biol *8*: 58-65, 1998.
4 Norton JD: ID helix-loop-helix proteins in cell growth, differentiation and tumorigenesis. J Cell Sci *113*: 3897-3905, 2000.
5 Riechmann V, van Cruchten I and Sablitzky F: The expression pattern of ID4, a novel dominant negative helix-loop-helix protein, is distinct from ID1, ID2 and ID3. Nucleic Acids Res *22*: 749-755, 1994.
6 Riechmann V and Sablitzky F: Mutually exclusive expression of two dominant-negative helix-loop-helix (dnHLH) genes, *ld4* and *ld3*, in the developing brain of the mouse suggests distinct regulatory roles of these dnHLH proteins during cellular proliferation and differentiation of the nervous system. Cell Growth Differ *6*: 837-843, 1995.
7 Murase R, Sumida T, Liu SH, Yoshimura T, Ishikawa A, Wei CF, Tano T and Hamakawa H: The expression and roles of ID1 and ID2 in the aggressive phenotype of human oral squamous cell carcinoma cells. J Oral Maxillofac Surg Med Pathol *25*: 12-17, 2013.
8 Sun XH, Copeland NG, Jenkins NA and Baltimore D: Id proteins Id1 and Id2 selectively inhibit DNA binding by one class of helix-loop-helix proteins. Mol Cell Biol *11*: 5603-5611, 1991.
9 Biggs J, Murphy EV and Israel MA: A human Id-like helix-loop-helix protein expressed during early development. Proc Natl Acad Sci USA *89*: 1512-1516, 1992.
10 Sun XH: Constitutive expression of the *Id1* gene impairs mouse B-cell development. Cell *79*: 893-900, 1994.
11 Melnikova IN, Bounpheng M, Schatteman GC, Gilliam D and Christy BA: Differential biological activities of mammalian ID proteins in muscle cells. Exp Cell Res *247*: 94-104, 1999.
12 Morrow MA, Mayer EW, Perez CA, Adlam M and Siu G: Overexpression of the helix-loop-helix protein ID2 blocks T-cell development at multiple stages. Mol Immunol *36*: 491-503, 1999.
13 Coppe JP, Itahana Y, Moore DH, Bennington JL and Desprez PY: ID-1 and ID-2 proteins as molecular markers for human prostate cancer progression. Clin Cancer Res *10*: 2044-2051, 2004.
14 Ishiguro A, Spirin KS, Shiohara M, Tobler A, Gombart, AF, Israel MA, Norton JD and Koeffler HP: ID2 expression increases with differentiation of human myeloid cells. Blood *87*: 5225-5231, 1996.
15 Noqueira MM, Mitjavila-Garcia MT, Le Pesteur F, Filippi MD, Vainchenker W, Kupperschmitt AD and Sainteny F: Regulation of ID gene expression during embryonic stem cell-derived hematopoietic differentiation. Biochem Biophys Res Commun *276*: 803-812, 2000.
16 Yokota Y, Mansouri A, Mori S, Sugawara S, Adachi S, Nishikawa S and Gruss P: Development of peripheral lymphoid organs and natural killer cells depends on the helix-loop-helix inhibitor Id2. Nature *397*: 702-706, 1999.
17 Parrinello S, Lin CQ, Murata K, Itahana Y, Singh J, Krtolica A, Campisi J and Desprez PY: ID-1, ITF-2, and ID-2 comprise a network of helix-loop-helix proteins that regulate mammary epithelial cell proliferation, differentiation, and apoptosis. J Biol Chem *276*: 39213-39219, 2001.
18 Iavarone A, Garg A, Lasorella A, Hsu J and Israel M: The helix-loop-helix protein ID2 enhances cell proliferation and binds to retinoblastoma protein. Genes Dev *8*: 270-284, 1994.
19 Kim J, Hong SJ, Park JY, Park JH, Yu YS, Park SY, Lim EY, Choi KY, Lee EK, Paik SS, Lee KG, Wang HJ, Do IG, Joh HW, Kim DS; Korea Cancer Biomarker Consortium: Epithelial–mesenchymal transition gene signature to predict clinical outcome of hepatocellular carcinoma. Cancer Sci *101*: 1521-1528, 2010.
20 Frewer KA, Sanders AJ, Owen S, Frewer NC, Hargest R and Jiang WG: A role for WISP2 in colorectal cancer cell invasion and motility. Cancer Genomics Proteomics *10*: 187-196, 2013.
21 Zhou JP, Gao ZL, Zhou ML, He MY, Xu XH, Tao DT, Yang CC and Liu LK: Snail interacts with ID2 in the regulation of TNF-α-induced cancer cell invasion and migration in OSCC. Am J Cancer Res *5*: 1680-1691, 2015.
22 Chang C, Yang X, Pursell B and Mercurio AM: ID2 complexes with the SNAG domain of SNAI1 inhibiting SNAI1-mediated repression of integrin β4. Mol Cell Biol *33*: 3795-3804, 2013.
23 Villarejo A, Cortés-Cabrera A, Molina-Ortíz P, Portillo F and Cano A: Differential role of SNAIL1 and SNAIL2 zinc fingers in E-cadherin repression and epithelial to mesenchymal transition. J Biol Chem 289: 930-941, 2014.

Received June 15, 2016
Revised July 20, 2016
Accepted July 21, 2016